

Irreversibility analysis of R407A and R407C as alternatives of R22 in window type air conditioner

AYAD KHUDHAIR AL-NADAWI *

Middle Technical University (MTU), Institute of Technology-Baghdad,
Electronic Technologies Department, Iraq

Abstract Irreversibility analysis was investigated by using refrigerants R22, R407A, and R407C in window type air conditioner system. The experimental study was conducted at various ambient temperatures and air volumetric flow rates to determine the parameters that cause the energy degradation of the system. The irreversibility was compared with respect to volumetric flow rates of the air passing through evaporator (14.15, 12.74, and 10.618 m³/min) and different ambient temperatures (ranging from 28 °C to 39 °C dry bulb). Results show that the total irreversibility increases with refrigerant mass flow rate and ambient temperature for the three refrigerants. Additionally, R22 shows the highest irreversibility in low ambient temperature (28 °C to 30 °C) while R407A shows the lowest one with ambient temperature ranging from 30 °C to 36 °C. Both tested refrigerants are very good replacement for R22 in terms of irreversibility and energy analysis and these results are more remarkable with R407A.

Keywords: R407C; R407A; ODP; Window type air conditioner; Irreversibility analysis

Nomenclature

COP	–	coefficient of performance
C_p	–	specific heat at constant pressure, kJ/kgK
GWP	–	global warming potential
h	–	specific enthalpy, kJ/kg
i	–	current, A

*Email: ayadalnadawi@gmail.com

I	–	irreversibility
\dot{m}	–	mass flow rate, kg/s
P	–	pressure, MPa
p	–	power, kW
PAT	–	process average temperature, K
Q	–	capacity, kW
q	–	refrigeration effect, kJ/kg
s	–	specific entropy, kJ/kgK
T	–	temperature, K
V	–	voltage, V

Subscripts

a	–	air
ai	–	air in
ao	–	air out
c	–	condenser
cap	–	capillary
$comp$	–	compressor
e	–	evaporator
r	–	refrigerant
s	–	system
1	–	evaporator outlet
2	–	condenser inlet
3	–	condenser outlet
4	–	evaporator inlet

Abbreviations

CFC	–	chlorofluorocarbon
HCFC	–	hydrochlorofluorocarbon
ODP	–	ozone depletion potential
RAC	–	room air conditioning

1 Introduction

One of the most important issues that refrigeration industry faces recently is the growing global warming and greenhouse effect. The critical influence of the refrigeration industry on global warming has become a challenge to many researchers. Therefore, a large amount of efforts has been spent by researchers to meet the conditions of the Montreal Protocol. Hydrochlorofluorocarbons (HCFCs) and chlorofluorocarbons (CFCs) refrigerants have phased out at an increasing pace since September 1987. According to Montreal Protocol, CFC used mainly in refrigeration and air conditioning equip-

ment, was expected to phase out by 1996 in the developed countries. Developed countries will phase out HCFC by 2030 while developing countries will phase out HCFC by 2040 [1].

To deal with the above-mentioned situation for the air-conditioning and refrigeration systems, recently, R407C and R407A are nominated as one of the alternatives of R22, due to their zero ozone depletion potential (ODP), preferable thermodynamic properties, high performance improvement potential, and for easy redesign of the old equipment. However, side by side with finding new alternative refrigerants, we have to use the available equipment more effectively. By means of the irreversibility analysis, we can determine the factors that can cause the inefficiencies in any refrigeration system.

Generally speaking, refrigeration systems have traditionally been analyzed by the first law of thermodynamics. This type of analysis deals with the quantity of energy and not quality. Irreversibility analysis deals with the quality of the energy which allow engineers to re-examine the existing energy conversion cycles and new working fluids with respect to cycle losses and the cycle component inefficiencies. Irreversibility analysis uses the second law of thermodynamics together with the first law of thermodynamics for design, analysis and improvement of the systems. It provides a measurement of the degradation of efficiencies in the system and the true location of these in efficiencies. It can help also to use the available resources more effectively. Therefore, we can determine the factors or conditions that cause the degradation of energy or inefficiencies in any energy system.

Most studies related to the refrigeration cycle in the open literatures have been generally based on the application of the first law of thermodynamics. Recently, good attention was paid to the irreversibility analysis due to its importance. Kilicarslan and Muller, presented irreversibility analysis for vapor compression cascade refrigeration system [2]. Refrigerant mixtures R12-R13, R22-R13, R134a-R13, and R404a-R13 were studied. The study show that refrigerant mixture R12-R13 has the lowest irreversibility while R404a-R13 has the highest one. Bolaji and Bukola studied experimentally the exergetic performance of a domestic refrigeration system using R12, R134a, and R152a [3]. The results showed that the highest exergetic efficiency was obtained using R152a. Also, the average values of exergy of the system using R134a and R152a are 13.6% lower and 4.4% higher than that of R12, respectively. Ahmed *et al.* [4], has performed exergy analysis in compression refrigeration system using R600, R600a, and R290.

It is found that hydrocarbons (R600a) have 50% higher exergy efficiency than R134a. Also, the results showed that the mixture of hydrocarbons have the best performance based on the exergy analysis. Stanciu *et al.* [5], presented exergy analysis and exergy destruction for one stage vapor compression refrigeration system for five refrigerants (R22, R134a, R717, R507a, and R404a). The results show that ammonia presents the highest value of irreversibilities. Also, the highest exergy destruction rate is in the compressor for R134A, R717 and almost for R22. In turn, Alshatti presented a model to simulate a variable refrigerant flow (VRF) air conditioning system using R22 and R134a under different cooling conditions [6]. Also, it provided a mathematical model that covers the mass, energy, entropy and exergy balances of a typical air conditioning system. The results indicate that an air conditioning system is quite sensitive to air properties, sensible and latent cooling loads.

Atharva and Lorenzo, introduced an experimental comparison of the drop-in energy performance and capacities of refrigerants R1234yf and R32 in the R410A heat pump split system for ducted heating, ventilation, and air conditioning (HVAC) in residential applications [7]. The experiments were conducted for cooling and heating mode of the unit and the outdoor temperature was varied from -8°C to 46°C . The results show that R32 has comparable heating and cooling capacities as those for R410A and also similar coefficients of performance (COPs). Further, refrigerant R1234yf provided similar COPs as R410A but this refrigerant had rather low capacities with respect to those for R410A. Jarahnejad presented two newly developed refrigerants, R1234yf and R1234ze as promising drop-in replacements for the common high global warming potential (GWP) [8]. R134a and R1234yf were investigated experimentally while R1234ze was investigated theoretically. The results show that R134a has respectively 2–9.2% and 4.4–15% higher COP as well as 0–3% and 0–3.8% higher volumetric cooling capacity than R1234yf at condensing temperatures of 30°C and 40°C . Further, the COP of R1234ze is about 1% lower than R134a and it is about 3% higher than R1234yf as well. The cycle performance of the binary mixture R32/R1234yf and the ternary mixture R744/R32/R1234yf were experimentally carried out and compared for their compositions corresponding to GWP of 200 and 300, Fukuda *et al* [9]. Further, irreversible losses in each element are discussed on the experimental data that changing heat sink water temperature of condensation inlet and outlet. irreversible loss in heat exchanger increases because of lower heat transfer performance

of heat exchanger.

Hao *et al.* [10], performed energy and exergy analysis of a refrigeration system with vapor injection. Results indicate that injection system can reduce exergy loss system. Yadav and Sharma performed exergy analysis of vapor compression refrigeration tutor using R134a as a refrigerant. The results stated that the maximum exergy destruction is in condenser. Aprea *et al.* [12] have conducted the experimental study of drop-in substitution of R134a with pure R1234yf, the mixture R1234yf/R134a (90/10% in weight), pure R1234ze and the mixture HFO1234ze/R134a (90/10% in weight) in a domestic refrigerator. The results show that the indirect contribution of the new refrigerants to global warming is smaller than that of R134a. Dudar *et al.* [13] presented the possible exergy efficiency increase of two-phase ejector refrigeration compression cycle with various working fluids and various operating conditions: R134a, R507, R290, R600a, and R717. The results prove that there is improvement of the efficiency of the compression refrigeration cycle even for low-pressure refrigerants, e.g., isobutene. The authors attributed this behavior to the complete reduction of the exergy losses occurring in the throttling valve and low losses produced in the compressor. Kumar and Gupta introduced the experimental performance analysis of a window air conditioner using R22 and R410A [14]. The test results show that the compressor power of R410A is higher than that of R22 and the average COP of R410 is lower than that of R22 refrigerant.

From the above mentioned literature survey, it is obvious that most of the studies related to the irreversibility analysis focused on domestic refrigerator, and vapor compression refrigeration system in general. Also, some of the compression refrigeration system have been based on a theoretical compression refrigeration cycle in which the effects of subcooling, superheating, pressure losses, and ambient temperature were not taken into consideration. However, the present study is different from the studies in the literature because a detailed irreversibility analysis for R22, R407A, and R407C was done experimentally to room air conditioner (RAC). Further, volumetric flow of the air passing through the evaporator and ambient temperature were taken into consideration.

Lots of new blends and refrigerants are being introduced to substitute conventional refrigerants and many studies were done for that purpose. To achieve the best thermodynamic properties, performance, and low ODP, two zeotropic refrigerants were introduced to be tested as alternative refrigerants to R22 in the window type air conditioner system. These re-

refrigerants were R407C comprising of R32/R125/R134a in a mass fraction composition percentage as 23/25/52 respectively, and R407A is of the refrigerants R32/R125/R134a with 20/40/40 mass fraction percentage. The main difference between the pure and zeotropic refrigerant is the difference in boiling point of their component due to the difference of vapor and liquid mass fraction at equilibrium [15]. Table 1 compares some characteristics of selected and common refrigerants.

Table 1: Comparing properties of different refrigerants.

Refrigerants	Chemical composition	Critical temperature (°C)	Critical pressure (MPa)	Normal boiling point (°C)	Temperature glide		ODP	GWP
					8 °C	45 °C		
R22	CHClF ₂	96.10	4.990	-29.75	0.00	0.00	0.055	1810
R407C	CH ₂ F ₂ , CF ₃ CHF ₂ , CH ₂ FCF ₃	86.10	4.650	-43.00	7.90	4.70	0.0	1800
R407A	CH ₂ F ₂ , C ₂ HF ₅ , CH ₂ FCF ₃	83.00	4.540	-45.50	5.50	4.00	0.0	2100
R410A	CH ₃ F ₂ , CHF ₂ CF ₃	71.36	4.900	-51.44	0.11	0.11	0.0	2088
R134a	CH ₂ FCF ₃	101.06	4.059	-26.07	0.00	0.00	0.0	1430
R143a	CF ₃ CH ₃	72.70	3.800	-47.24	0.00	0.00	0.0	4300

The present study is based on the second law of thermodynamics in which the irreversibility analysis was carried out in room air conditioner system (RAC). The experimental study was done with various ambient temperatures and three volumetric flow rates of the air passing through evaporator (14.15, 12.74, and 10.618 m³/min) to determine the parameters that cause the energy degradation of the system. Three refrigerants, namely R22, R407A, and R407C were charged into the system and then the measurements for each refrigerant at different air volumetric flow rates and ambient temperature were collected.

2 Description of the experimental setup

The experimental work of Al-Nadawi will be recalled [16]. A schematic diagram of the experimental apparatus is shown in Fig.1. The RAC system was originally designed to work with R22. The main modification to the system is the addition of measuring devices.

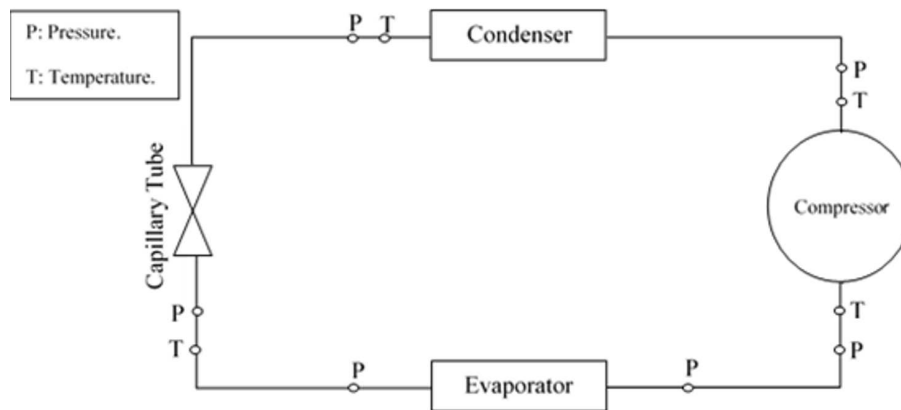


Figure 1: Schematic diagram of experimental apparatus.

The test rig consists of:

- reciprocating type piston compressor with $0.21 \text{ m}^3/\text{min}$ theoretical displacement volume, and 3GS mineral oil;
- finned tube evaporator and condenser, the characteristic and physical dimensions of evaporator and condenser;
- three capillary tubes (0.76 m length, 0.001 mm inner diameter for each one).

The evaporator and condenser are made from copper tubes and louvered fins, Tab. 2. The evaporator has three separate circuits which don't rejoin until the evaporator exits whereas; the condenser has three circuits in three rows and these circuits are brought together to form the fourth row as shown in Fig. 2. The test rig is suitably modified to connect temperature, and pressure gauges. Additionally, all pipelines were insulated to insure that there is no heat gain or loss between the pipe lines and its surroundings. The instruments of measurements details can be found in [16].

The measurements were taken at each air volumetric flow rates, ambient temperature, and for each refrigerant after the system had been fully stabilized. The refrigerant side measurements (temperature and pressure) and air side measurements (dry and wet bulb temperature) are recorded and collected. These data are collected at different ambient temperatures (ranging from 28°C to 39°C dry bulb) to investigate the effect of the environmental conditions on the performance and irreversibility of the RAC unit, the data collected are:

Table 2: The characteristic physical dimensions of evaporator and condenser [16].

Dimension specification	Unit	Evaporator	Condenser
Tube length	mm	380	560
Dimension (L×W×H)	mm	380×90×380	560×45×400
No. of circuits		3	3
No. of rows		4	4
No. of tubes		57	80
Tube outside diameter	mm	9.5	7.9337
Tube inside diameter	mm	7.8994	6.22
Tube material		copper	copper
Tube metal thermal conductivity	W/m K	386	386
Inner tube surface		smooth	smooth
Transverse tube pitch	mm	22.3	18.65
Longitudinal tube pitch	mm	22.3	18.65
Fin thickness	mm	0.235	0.137
Fin pitch	mm	2	1.5
Total No. of fin		174	342
Fin type		louvered	louvered
Fin metal		aluminium	aluminium
Fin thermal conductivity	W/m K	202	202
Area of heat exchanger	m ²	11.13	10.75
Area of fin	m ²	10.4	9.608
Area of tube	m ²	0.7147	1.144776

- refrigerant temperature at inlet and outlet of the evaporator,
- refrigerant temperature at inlet and outlet of the condenser,
- pressure at inlet and outlet of the evaporator on the refrigerant side,
- pressure at the suction line of the compressor,
- pressure at inlet and outlet of the condenser,
- pressure at outlet of the capillary tube,
- dry and wet bulb temperatures at inlet and outlet of each evaporator and condenser,
- the current and voltage are measured for RAC unit.

This procedure is repeated at the same ambient condition when the volumetric flow rates of the air passing through evaporator are 14.15, 12.74, and 10.618 m³/min. The test began at highest air volumetric flow rates then stepped down to the lowest value. This is done to show the effect of changing the volumetric flow rate of air on the performance and irreversibility of

the RAC. To maintain stability of the RAC, the system was run at least 10 min prior to each test condition.

On the other hand, a detailed analysis of the experimental uncertainties was done. The following equation was used to calculate the uncertainties for the experimental values:

$$Q = f(Z_1 \dots, Z_n), \quad (1)$$

$$\left(\frac{u_q}{q_e}\right)^2 = \sum_{i=1}^N \left(\frac{u_{Z_i}}{Z_i}\right)^2, \quad (2)$$

$$U = k u_q, \quad (3)$$

where Q is the discrete value, Z_i is the input quantity, U is the expand uncertainty, k is the converge factor, u_q is the standard uncertainty, q_e is the best estimate quantity, and u_{Z_i} is the standard uncertainty of input quantity.

For 98% degree of confidence level ascribed to the true value of Q being inside the interval, k will be taken as 2.327 [17]. From calibration it was found that the maximum error of all pressure gauge tested was ranged between (-0.034 to 0.13 MPa) and maximum error in temperature reading was 3 °C. This analysis revealed that the maximum for typical uncertainties was estimated to be 1% for COP and 1.8% for irreversibility.

3 Experimental data analysis

Qualitative and quantitative information were gained from around 159 data points obtained in this study. Performance and irreversibility analysis were done to the experimental data to address the effect of ambient temperature, air volumetric flow rates, and refrigerant type on the system irreversibility.

3.1 Performance analysis

This study continued by calculation of cycle irreversibility of zeotropic refrigerants, namely R407C and R407A, and pure refrigerant R22. Moreover, an experiment has been done in the RAC test rig to compare the experimental cycle performance of R22, R407C, and R407A. The pressure-enthalpy ($P-h$) and the temperature-entropy ($T-s$) diagrams of refrigeration system are shown in Fig. 2.

The following assumptions are considered:

- air temperature at the entrance and exit of heat exchangers are constant and homogenous at all tubes,
- mass flow rate of refrigerant is constant at all parts of the RAC unit,
- enthalpy change in the capillary tube is negligible,
- steady-state and uniform flow conditions exist through the elements of system,
- compressor process in the compressor is adiabatic.

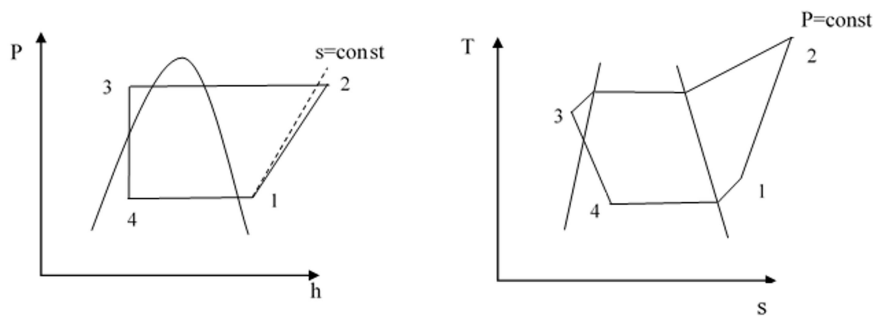


Figure 2: P - h and T - s diagrams for the refrigeration cycle.

The refrigerating effect accomplished by the RAC evaporator can be stated as

$$q_{evap} = h_1 - h_4, \quad (4)$$

where, h_1 and h_4 are the the specific enthalpies at evaporator outlet and inlet, respectively.

The evaporator capacity can be calculated from the air side process as

$$Q_{evap} = \dot{m}_a(h_{ai} - h_{ao}), \quad (5)$$

where \dot{m}_a , h_{ai} and h_{ao} are the air mass flow rate, and inlet and outlet values and the specific enthalpies across the evaporator, respectively. Enthalpy of air was calculated by using the correlator presented by Tarrad and Shehhab [18].

The refrigerant circulated mass flow rate was calculated by

$$\dot{m}_r = \frac{Q_{evap}}{q_{evap}}. \quad (6)$$

The compression process was assumed to be adiabatic and the power was calculated from the current (i), voltage (V) and the power factor ($\cos \phi$)

$$p = iV \cos \phi . \quad (7)$$

Here the power factor was assumed to be unity. Finally, COP can be calculated from the following:

$$\text{COP} = \frac{Q_{evap}}{p} . \quad (8)$$

3.2 Irreversibility analysis

Irreversibility analysis is based on a simple vapor refrigeration system cycle used in air conditioning and refrigeration industry. Irreversibility of the system consists of the irreversibility of compressor, capillary tube, evaporator and condenser. It can be written as

$$I_s = I_{comp} + I_{cap} + I_e + I_c , \quad (9)$$

where I_{comp} , I_{cap} , I_e , and I_c are rate of the irreversibility of the compressor, capillary tube, evaporator, and condenser, respectively. The system analysis of the current study is based on steady state steady flow process. Irreversibility of the compressor can be written as follows:

$$I_{comp} = \dot{m}_r T_0 (s_2 - s_1) , \quad (10)$$

where T_0 is the environment temperature, \dot{m}_r , s_1 and s_2 are the refrigerant mass flow rate flowing through system and the specific entropies across compressor, respectively. The main source of irreversibility during expansion process can be attributed to the sudden expansion of refrigerant. Irreversibility of capillary tube can be expressed as

$$I_{cap} = \dot{m}_r T_0 (s_4 - s_3) , \quad (11)$$

where s_3 is the specific entropy at the thermal expansion valve inlet and s_4 is the specific entropy at the outlet.

The main reason of irreversibility in the evaporator is heat transfer through the finite temperature difference between the refrigeration space and evaporator. Not to mention that the degree of superheating space also affects the irreversibility of the evaporator. Also, the rate of irreversibility

in a condenser is caused by the heat transfer between the condenser and its condensing environment at a finite temperature difference. To calculate the rate of irreversibility for the evaporator and condenser, we need to calculate the process average temperature (PAT) for evaporator and condenser. In terms of measurable thermodynamic variables, the PAT is given by [19]

$$\text{PAT} = \frac{\int_{in}^{out} dh}{\sum_{i=1}^n \frac{\int dh}{T}}, \quad (12)$$

where n indicates the relevant heat exchangers piecewise cycle branches. The PAT can be interpreted as the temperature of the refrigerant were the process to be viewed as an equivalent isothermal process, for purposes of calculating irreversibility. As such, the PAT is not a measured temperature; rather it is the proper reference temperature for evaluating dissipative losses [19].

The rate of irreversibility for evaporator is calculated using the formula

$$I_e = \dot{m}_r T_0 \left[(s_1 - s_4) - \frac{(h_1 - h_4)}{\text{PAT}_e} \right], \quad (13)$$

where PAT_e is the process average temperature for evaporator. Similarly, the rate of irreversibility for condenser is calculated as follow:

$$I_c = \dot{m}_r T_0 \left[(s_3 - s_2) - \frac{(h_3 - h_2)}{\text{PAT}_c} \right], \quad (14)$$

where PAT_c is the process average temperature for condenser.

The data collected by Al-Nadawi will be recalled [16]. Furthermore, a C++ code, based on the lumped parameter model, was developed to calculate all of the equations mentioned previously. The properties of the refrigerants, namely R22 and R407C, are obtained from the published data by *ASHRAE Hand Book* [20] and the thermodynamic properties of R407A were obtained from Ineos Flour Company [21] with curve fit equations obtained by lab fit program and commercial numerical computing environment Matlab [22] for the three refrigerants.

4 Flowchart

The flow chart for generating the $P-h$ and $T-s$ diagrams is shown in Fig. 3. The enthalpy and entropy of each condition has been gained by means of

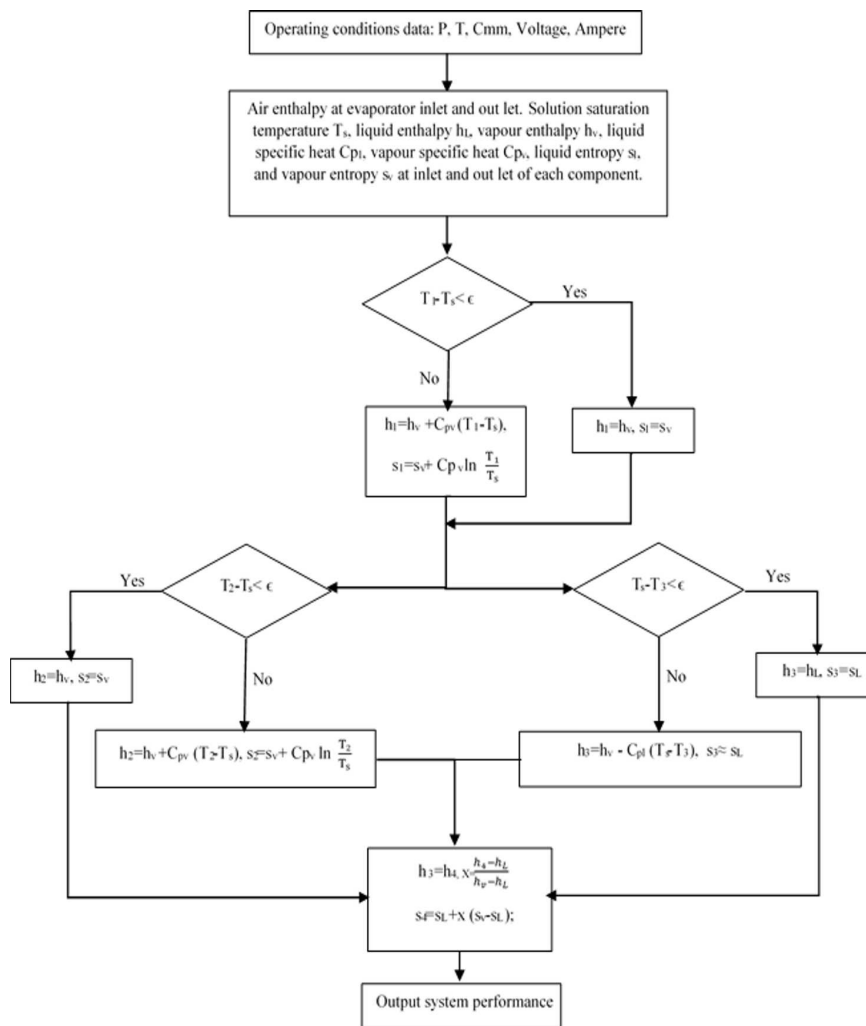


Figure 3: Flowchart for calculating the system irreversibility (ϵ – error, $\epsilon = 0.005$).

C++ computer code built for this purpose. The source code consists of the main program with two functions to calculate the property of air and refrigerants. For certain operating conditions, different thermodynamic properties are calculated to obtain enthalpies and entropies at inlet and outlet of the evaporator and then the procedure is repeated for compressor, condenser and capillary tube. Also, air enthalpies were calculated to calculate the evaporator capacity. After that, Eqs. (4) to (14) are applied

in order to calculate the irreversibility of the system.

5 Results and discussion

By means of the C⁺⁺ computer code developed, the data collected during the present work is investigated. The parameters used to assess the irreversibilities are ambient temperature, mass flow rate of the refrigerants, I_s , $\frac{I_s}{Q_{evap}}$, the refrigerant type, air volumetric flow rate and the process average temperature for the evaporator and condenser. It is worthy to mention that the experimental analysis was done to actual refrigeration circuit installed in the window type air conditioner system. Therefore, the data extracted from the experimental tests may show some spreads because there is many variables that could affect the results.

The variation of the irreversibility of the system with the ambient temperatures and for the air volumetric flow rates of 14.15, 12.74, and 10.618 m³/min for R22, R407C, and R407A, is shown in Fig. 4. Clearly,

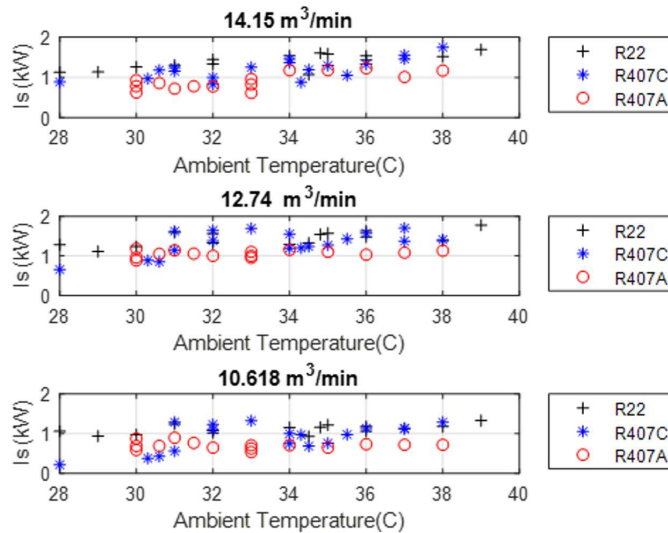


Figure 4: Variation of I_s as a function of ambient temperature for R22, R407C, and R407A.

the total irreversibility of the system increases with ambient temperatures for R22, R407C, and R407A. It can be concluded from the figure that the R22 show the highest irreversibility in low ambient temperature (28 °C

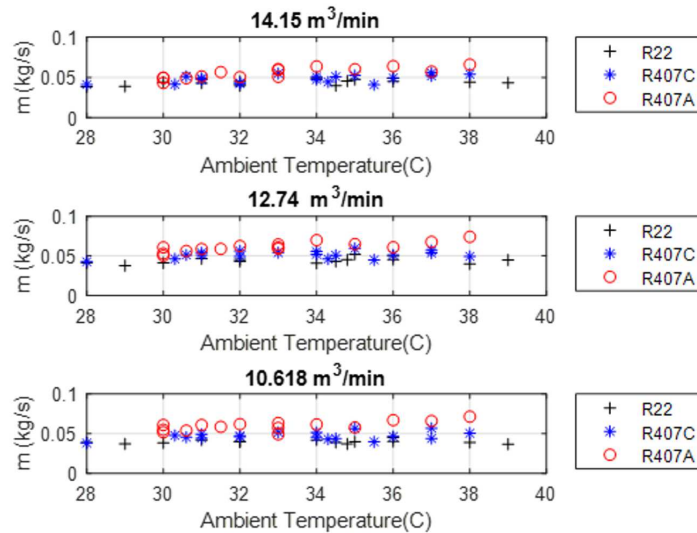


Figure 5: Variation of refrigerant mass flow rate as a function of ambient temperature for R22, R407C, and R407A.

to 30 °C) for all three air volumetric flow rates. For 14.15 m³/min, R22 show the highest irreversibility, while R407A show the lowest one with ambient temperature ranging from 30 °C to 36 °C. After that, R407C show increasing trend with respect to R22, and R407A. On the other hand, R22 and R407C illustrate almost the same magnitude at ambient temperature ranging from 30 °C to 36 °C. For the flow rate equal 12.74 m³/min, it is obvious that R407A has the lowest irreversibility. Whereas, the irreversibility of R22 is dominant at low ambient temperature. Additionally, the total irreversibility of R22 and R407C are almost the same at medium and high ambient temperature for 10.618 m³/min. On the other hand, R407A show the lowest irreversibility for 10.618 m³/min. The general trend of the total irreversibility can be attributed to the effect of refrigerant mass flow rate, PAT_e and PAT_c as shown in Figs. 5, 6, and 7.

When the ambient temperature increases the refrigerant mass flow rate increases as well and hence that affect the rate of irreversibility of the system, Fig. 5. Also, it is obvious that the refrigerant mass flow rate shows an increasing trend with increasing ambient temperature and the largest refrigerant mass flow rate occur in R407A for all three air volumetric flow rates. The increasing trend explains the behaviour of total irreversibility

with increasing ambient temperature as shown in Fig. 4. However, R407C and R22 have almost the same refrigerant mass flow rate with small difference. Therefore, refrigerant mass flow rate behaviour can explain the general increasing trend of total irreversibility.

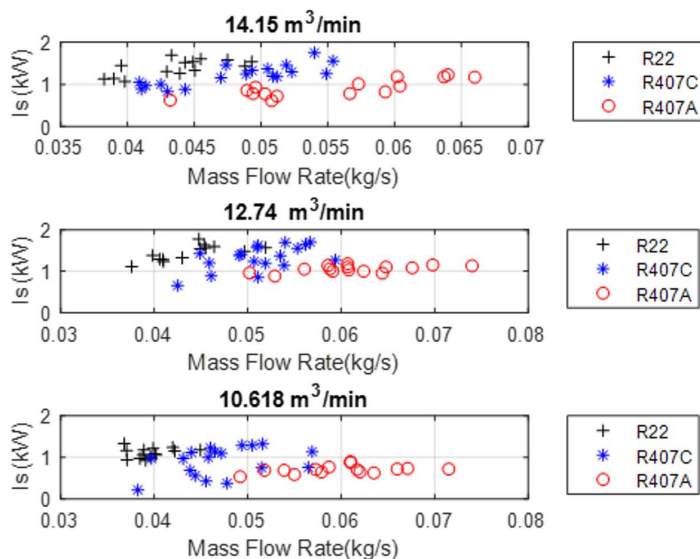


Figure 6: Variation of I_s as a function of refrigerant mass flow rate for R22, R407C, and R407A.

Moreover, the total irreversibility was illustrated as a function of mass flow rate as shown in Fig. 6. Here, as the refrigerant mass flow rate increase, the total irreversibility increases as well for the three refrigerants at 14.15, 12.74, and 10.618 m^3/min . Again, this behavior can explain the behavior of total irreversibility when the ambient temperature increases. That is, the refrigerant mass flow rate increases with increasing ambient temperature and hence the total irreversibility increases as well. Additionally, R22 show the lowest value of refrigerant mass flow rate and the highest value of total irreversibility. On the other hand, R407A mass flow rate show almost increasing linear trend.

The process average temperature of the evaporator and condenser with respect to the ambient temperature for R22, R407C, and R407A, are shown in Figs. 7 and 8, respectively. As the ambient temperature increases, the process average temperature for evaporator and condenser increases for the three refrigerants and volumetric flow rates of 14.15, 12.74, and 10.618 m³/min. As a result, the rate of the irreversibilities of the system increase. The figure stated clearly that R407A refrigerant has the lowest PAT_e and as a result of that the total irreversibility will decrease, Fig 4. Further, R407C and R407A have approximately both same values of evaporator process average temperature PAT_e at 14.15 and 12.74 m³/min. Similarly, condenser process average temperature PAT_c shows the same trend, Fig 8. One can observe that PAT_c increases with increasing ambient temperature for the three refrigerants and 14.15, 12.74, and 10.618 m³/min. Again, this behavior can lead to increase in the total irreversibility, Fig. 4. Additionally, R407A has the lowest PAT_c which confirm the results illustrated in Fig. 4.

It is worthy to investigate the effect of combined ratio $\frac{I_s}{Q_{evap}}$, Fig. 9. This term can give the relation between Q_{evap} and I_s with increasing ambient temperature. It is clear from the figure that $\frac{I_s}{Q_{evap}}$ increased with increasing ambient temperature. It means that Q_{evap} decreased with high ambient temperature and as a result of that $\frac{I_s}{Q_{evap}}$ will increase. This trend is very obvious with R22 and R407C but not in the case of R407A, which means that Q_{evap} and I_s have the same effect on the RAC. In Fig. 10 is reported $\frac{1}{COP}$ against $\frac{1}{Q_{evap}}$ for R22, R407C, and R407A. Obviously, as $\frac{1}{Q_{evap}}$ increase, $\frac{1}{COP}$ increase as well for R22, R407C, and R407A. Comparing the volumetric flow rate for the three refrigerants, one can observe that the general trends are very similar. However, this trend is more remarkable with 14.15, and 10.618 m³/min. The general behavior is justified by the greater refrigerant mass flow rate for high ambient temperature and for R407A. Which means that R407A has the higher COP and the lower irreversibility. One can say that R407C, and R407A are very good replacement for R22 in terms of irreversibility and energy analysis and these results are more remarkable with R407A.

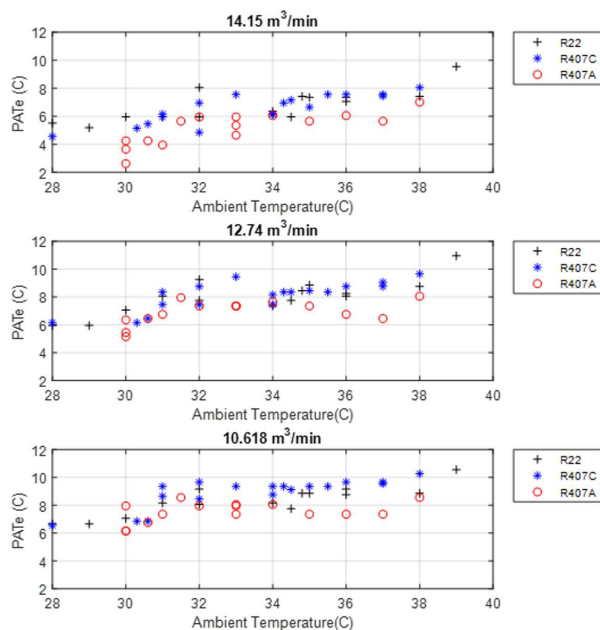


Figure 7: Variation behavior of PAT_e with the ambient temp. for R22, R407C, and R407A.

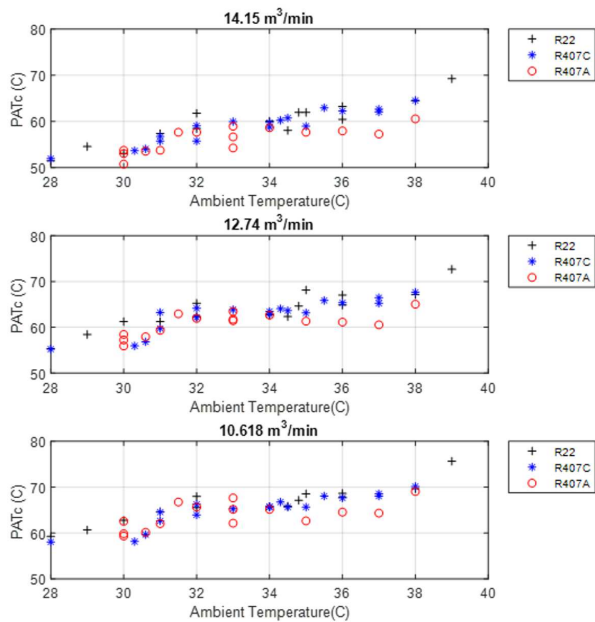


Figure 8: Variation behavior of PAT_c with the ambient temp. for R22, R407C, and R407A.

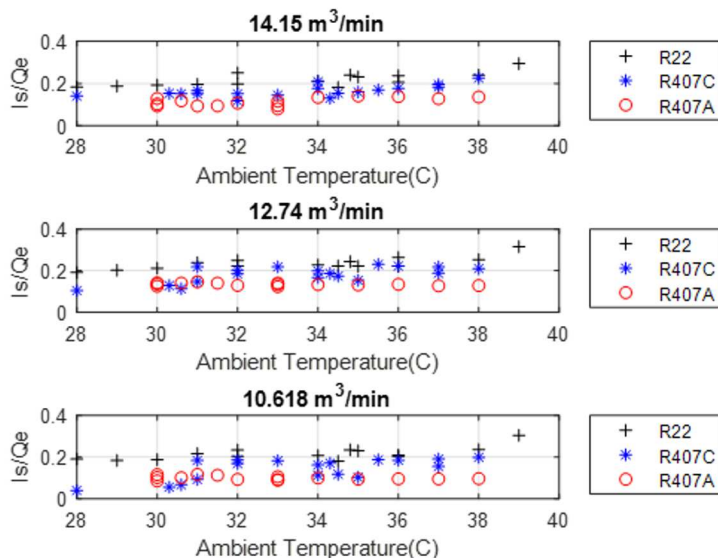


Figure 9: $\frac{I_s}{Q_e}$ as a function of ambient temperature for R22, R407C, and R407A.

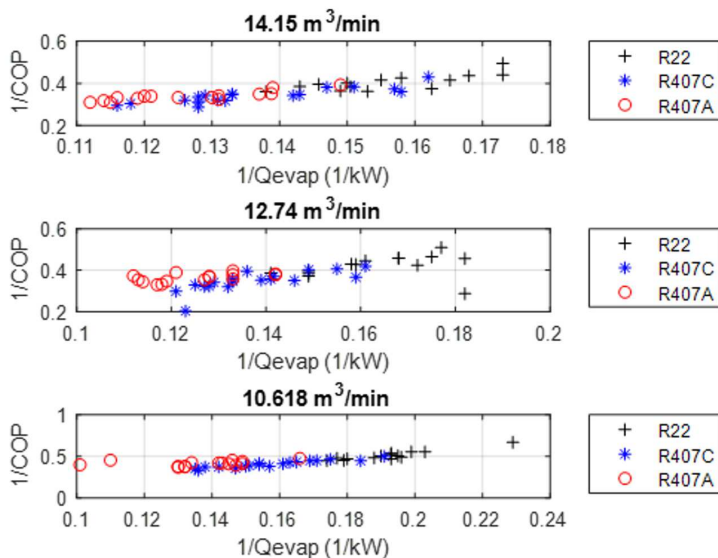


Figure 10: $\frac{1}{COP}$ against $\frac{1}{Q_{evap}}$ for R22, R407C, and R407A.

6 Conclusions

The following conclusions have been drawn from the research:

- the total irreversibility of the system increases with ambient temperatures for R22, R 407C, and R407A,
- R22 show the highest irreversibility in low ambient temperature (28 °C to 30 °C) while R407A show the lowest one with ambient temperature ranging from 30 °C to 36 °C,
- the total irreversibility increases when the refrigerant mass flow rate increase for the three refrigerant. However, R407A show the lowest irreversibility and highest mass flow rate and this can lead to increase the system efficiency,
- R407C and R407A are very good replacement for R22 in terms of irreversibility and energy analysis and these results are more obvious with R407A.

Received 27 November 2018

References

- [1] VERMA J.K., SATSANGI A., CHATURANI V.: *A review of alternative to R134a (CH₃CH₂F) refrigerant*. IJETAE **3**(2013), 1, 300–304.
- [2] KILICARSLAN A., MULLER N.: *Irreversibility analysis of a vapor compression cascade refrigeration cycle*. In: Proc. ASME Int. Mech. Eng. Cong. Exp., Oct. 31–Nov. 6, 2008, Vol. 8: Energy Systems: Analysis, Thermodynamics and Sustainability; Sustainable Products and Processes. Boston, Massachusetts, USA. Oct. 31–Nov. 6, 2008, pp. 517–522. ASME. <https://doi.org/10.1115/IMECE2008-66363>.
- [3] BOLAJI B.O.: *Energetic performance of a domestic refrigerator using R12 and its alternative refrigerants*. J. Eng. Technol. Manage **5**(2010), 4, 435–446.
- [4] AHMED J.U., RAIDUR R., MASJUKI H.H.: *Prospect of hydrocarbon uses based on exergy analysis in the vapour compression refrigeration system*. In: Proc. IEEE 1st Conf. on Clean Energy and Technology CET, 2011.
- [5] STANCIU C., GHEORGHIAN A., STANCIU D., DOBROVICESCU A.: *Exergy Analysis and Refrigerant Effect on the Operation and Performance Limits of a One Stage Vapour Compression Refrigeration System*. Politetlnica University of Bucharest, Bucharest 2011.
- [6] ALSHATTI R.A.: *Analysis of Variable Refrigerant Flow and Exergy in Air Conditioning Systems*, MSc thesis, University of South Florida, Tampa 2011.

- [7] ATHARVA B., LORENZO C.: *Drop-in performance of low gwp refrigerants in a heat pump system for residential applications*. In: Proc. Int. Refrigeration and Air Conditioning Conf., 2012, paper 1211, <http://docs.lib.purdue.edu/iracc/1211>.
- [8] JARAHNEJAD M.: *New Low GWP Synthetic Refrigerants*. MSc thesis, KTH School of Industrial Engineering and Management Energy Technology, Stockholm 2012.
- [9] FUKUDA S., KOJIMA H., KONDOU C., TAKATA, N., KOYAMA S.: *experimental assessment on performance of a heat pump cycle using R32/R1234yf and R744/R32/R1234yf*. In: Proc. 16th Int. Refrigeration and Air Conditioning Conf., Purdue, July 11–14, 2016, paper 1651, <http://docs.lib.purdue.edu/iracc/1651>.
- [10] HAO T., ZHENG S.-X., YANG Y.-T., WANGD C. ZHAO Y.-X., HE S.-Y.: *Energy and exergy analysis of a refrigeration system with vapour injection using reciprocation piston compressor*. In: Proc. 2nd Int. Conf. on Sustainable Development, Advances in Engineering Research, **94**, 2016.
- [11] YADAV P., SHARMA A.: *exergy analysis of R134a vapour compression refrigeration tutor*, IOSR Journal of Mechanical and Civil Engineering (IOSR-JMCE), In: Proc. Nat. Conf. on Advances in Engineering, Technology & Management, AETM'15, 73–77, <http://www.iosrjournals.org>
- [12] APREA C., GRECO A., MAIORINO A.: *HFOs and their binary mixtures with HFC134a working as drop-in refrigerant in a household refrigerator. energy analysis and environmental impact assessment*. Appl. Therm. Eng. **141**(2018), 226–233.
- [13] DUDAR A., BUTRYMOWICZ D., ŚMIERCIEW K., KARWACKI J.: *Exergy analysis of operation of two-phase ejector in compression refrigeration system*. Arch. Thermodyn. **34**(2013), 4, 107–122.
- [14] KUMAR A., GUPTA R.: *A performance of a window air conditioner using alternative refrigerants R22 and R410A*. Int. J. Eng. Sci. Res. Technol. **2**(2013), 7, 1842–1848.
- [15] TARRAD A.H., ABBAS A.K.: *evolution of a proper alternative refrigerant for R-22 in air conditioning systems*. Emirates J. Eng. Res. **15**(2010), 2, 41–51.
- [16] AL-NADAWI A.K.: *Experimental and theoretical study of R407c and R407a as an alternative of R22 refrigerant in a window type air conditioner*. MSc thesis, College of Engineering, Al-Mustansiriya University, Baghdad 2010, https://www.researchgate.net/publication/327766514_Experimental_and_Theoretical_Study_of_R407C_and_R407A_as_an_Alternative_of_R22_Refrigerants_in_a_Window_Type_Air_Condition
- [17] LIRA I.: *Evaluating the Measurement Uncertainty-Fundamental and Practical Guidance*. Institute of Physics Publishing, 2002.
- [18] TARRAD A.H., SHEHHAB U.S.: *The prediction of environment effect on the performance of a vapor compression refrigeration system in air conditioning application*. Eng. Development J. **11**(2007), 1, 169–189.
- [19] GORDON J.M, NG K.C: *Cool Thermodynamics the Engineering, Diagnostic, and Optimization methods for Cooling Systems*, Chpt. 4. Cambridge International Science Publishing, 2001.
- [20] *ASHRAE Handbook—Fundamentals (SI)*, Chpt 30. American Society of Heating, Refrigerating and Air Conditioning Engineers, 2009.

- [21] *Thermodynamic Property Data for KLEA407A- British Units*. INEOS Fluor Company, 2008.
- [22] Matlab ver. https://www.mathworks.com/products/new_products/release_2017b.html